Inorganic Chemistry

Article

Conserved Mechanism of Copper Binding and Transfer. A Comparison of the Copper-Resistance Proteins PcoC from *Escherichia coli* and CopC from *Pseudomonas syringae*

Karrera Y. Djoko,[†,‡] **Zhiguang Xiao,*,†,‡ David L. Huffman,**[§] **and Anthony G. Wedd*,†,‡**

School of Chemistry, University of Melbourne, Parkville, Victoria 3052, Australia, Bio21
Molecular Science and Biotechnology Institute, 30 Flemington Road, Parkville,
Victoria 3010, Australia, and Department of Chemistry, Western Michigan University,
Kalamazoo, Michigan 49008-3842

Received January 22, 2007

The copper-resistance proteins PcoC from *Escherichia coli* and CopC from *Pseudomonas syringae* exhibit 67% sequence identity, but the chemistry reported for PcoC (Peariso, K.; Huffman, D. L.; Penner-Hahn, J. E.; O'Halloran, T. V. *J. Am. Chem. Soc.* **2003**, *125*, 342–343) was distinctly different from that reported for CopC (Zhang, L.; Koay, M.; Maher, M. J.; Xiao, Z.; Wedd, A. G. *J. Am. Chem. Soc.* **2006**, *128*, 5834–5850). The source of the inconsistency has been identified, and His1 is confirmed as an unprecedented bidentate ligand in each protein. Access to a bona fide wild-type PcoC protein allowed unequivocal observation of intermediates involved in intermolecular redox copper transfer reactions.

Introduction

Copper is a trace element required at the active sites of many essential enzymes. However, it is toxic in excess or in "free" forms inside the cell because of its ability to promote radical formation via Haber-Weiss and Fenton reactions and to coordinate randomly with functional groups. Biological systems have evolved regulation mechanisms that balance copper import and export to ensure proper nutrient levels while minimizing toxic effects. These mechanisms use trafficking proteins that mobilize copper ions specifically or eliminate them.[1,2]

Some strains of *Escherichia coli* can survive in copper-rich environments that would normally overwhelm the chromosomal copper-tolerance system.[3] Such strains possess additional plasmid-encoded genes that confer copper resistance. A well-documented example was found in the feces of copper-fed pigs, and its resistance was attributed to a plasmid-borne *pco* operon comprising seven genes, *pcoABCDpcoRSpcoE*.[4−6] High copper levels induce expression of proteins PcoABCDE that are regulated by the two-component system PcoRS.[5,7] The proteins operate in the periplasmic space to confer copper resistance.[6,8−10] PcoA, PcoC, and PcoE are soluble proteins, while PcoB and PcoD appear to be outer- and inner-membrane-bound copper pumps, respectively.[8,11]

Equivalent copper-resistance operons *copABCDcopRS* have been found in copper-resistant strains of *Pseudomonas syringae* pathovar *tomato* isolated from plants exposed to high levels of copper compounds and in strains of *Ralstonia metallidurans* isolated from sediments of a zinc decantation basin in Belgium.[9,12] The gene structures of the operons

* To whom correspondence should be addressed. E-mail: z.xiao@unimelb.edu.au (Z.X.), agw@unimelb.edu.au (A.G.W.). Fax: +61 3 9347 5180.
† University of Melbourne.
‡ Bio21 Molecular Science and Biotechnology Institute.
§ Western Michigan University.

(1) Pena, M. M.; Lee, J.; Thiele, D. J. *J. Nutr.* **1999**, *129*, 1251−1260.
(2) Huffman, D. L.; O'Halloran, T. V. *Annu. Rev. Biochem.* **2001**, *70*, 677−701.
(3) Rensing, C.; Grass, G. *FEMS Microbiol. Rev.* **2003**, *27*, 197−213.
(4) Tetaz, T. J.; Luke, R. K. *J. Bacteriol.* **1983**, *154*, 1263−1268.
(5) Rouch, D. A.; Camakaris, J.; Lee, B. T.; Luke, R. K. *J. Gen. Microbiol.* **1985**, *131*, 939−943.
(6) Brown, N. L.; Barrett, S. R.; Camakaris, J.; Lee, B. T.; Rouch, D. A. *Mol. Microbiol.* **1995**, *17*, 1153−1166.
(7) Rouch, D. A.; Brown, N. L. *Microbiology (Reading, U.K.)* **1997**, *143* (Part 4), 1191−1202.
(8) Lee, S. M.; Grass, G.; Rensing, C.; Barrett, S. R.; Yates, C. J.; Stoyanov, J. V.; Brown, N. L. *Biochem. Biophys. Res. Commun.* **2002**, *295*, 616−620.
(9) Cooksey, D. A. *FEMS Microbiol. Rev.* **1994**, *14*, 381−386.
(10) Puig, S.; Rees, E. M.; Thiele, D. J. *Structure* **2002**, *10*, 1292−1295.
(11) Huffman, D. L.; Huyett, J.; Outten, F. W.; Doan, P. E.; Finney, L. A.; Hoffman, B. M.; O'Halloran, T. V. *Biochemistry* **2002**, *41*, 10046−10055.
(12) Mergeay, M.; Monchy, S.; Vallaeys, T.; Auquier, V.; Benotmane, A.; Bertin, P.; Taghavi, S.; Dunn, J.; van der Lelie, D.; Wattiez, R. *FEMS Microbiol. Rev.* **2003**, *27*, 385−410.
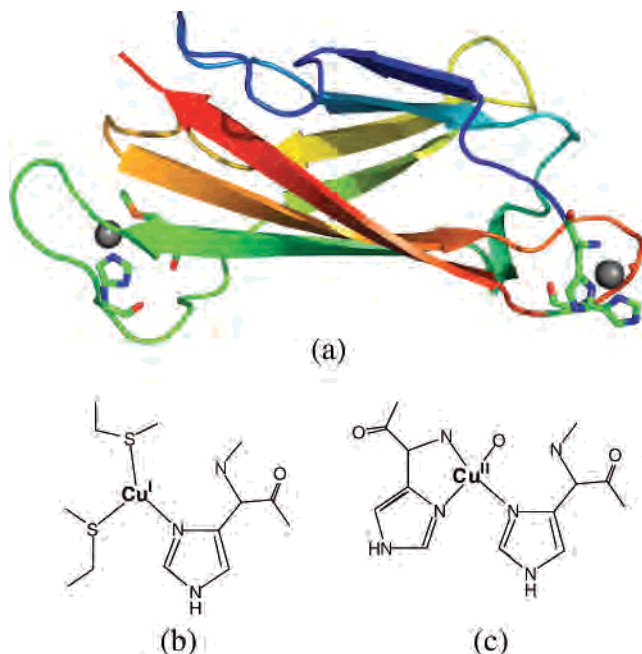
Figure 1. (a) Ribbon representation of PcoC and CopC proteins. 2D representation of (b) the Cu^I site and (c) the Cu^{II} site.

pco/copABCDRS are similar, as are the protein sequences, suggesting a conserved mechanism of copper resistance.

PcoC and CopC are small soluble proteins proposed to function as copper carriers in the periplasm. We and others have explored the fundamental chemistry of CopC from *P. syringae* pv. *tomato*.[13–17] The molecule is a β barrel with two separated binding sites specific for Cu^I and Cu^{II}: $[Cu^I(His)(Met)_{2,3}]$ and $[Cu^{II}(His)_2(N\text{-term})(OH_2)]$ (Figure 1). The latter features the amino terminus as a ligand, making His1 effectively a bidentate ligand,[17] a situation observed previously only in simple Cu^{II}-peptide complexes.[18–20] Production of variant proteins demonstrated that the two copper binding sites are interdependent. CopC effects intermolecular transfer from either site with or without a change of the oxidation state.[17] Such transfers require the availability of a high-affinity binding site to receive the transported ion. Overall, its properties are consistent with those expected of a versatile copper carrier interacting directly with other members of the Cop protein family to confer copper resistance.

The PcoC protein from *E. coli* has also been expressed and partially characterized.[11,21,22] PcoC and CopC have 67%

sequence identity (Figure 2), and they each bind both Cu^I and Cu^{II}. However, the chemistry observed for PcoC was distinctly different from that of CopC. Most importantly, Cu^I-PcoC was air-stable, while Cu^I-CopC reacted rapidly with dioxygen.

The differences have been traced to the presence of an additional N-terminal Ala residue in the PcoC protein as expressed.[11] Consequently, His1 was demoted to position 2, a situation that altered the nature of the Cu^{II} binding site dramatically. We have now generated the native form of PcoC and established the presence of His1 as a bidentate ligand in each protein. Access to a bona fide wild-type PcoC protein has allowed unequivocal observation of intermediates involved in intermolecular exchange of copper ions.

Materials and Methods

Plasmids and Site-Directed Mutagenesis. Plasmid pDLHII265 for overexpression of nA-PcoC (a variant protein with an Ala residue inserted before the native His1) was described previously.[11] Plasmid pDX905 for overexpression of a wild-type PcoC was constructed as follows. Two gene segments encoding the leader sequence of CopC from *P. syringae* and the protein sequence of PcoC from *E. coli* were amplified separately by PCR from plasmid templates pAT2[13] and pDLHII265 using T7 forward and reverse primers and a pair of overlapping primers that were designed based on the sequences of the joint sections of the two gene segments (Table S1 in the Supporting Information). The two resulting gene fragments were fused and amplified by PCR. This chimeric gene contained unique restriction sites *Xba*I and *Bam*HI and was doubly digested and ligated into a similarly digested pET20b(+) vector to create the expression plasmid pDX905 for a wild-type PcoC. Site-directed mutagenesis was carried out by PCR on the template pDX905 plasmid with overlapping primers that targeted the intended mutation site(s) (Table S1 in the Supporting Information). Each variant generated was confirmed by DNA sequencing.

Protein Expression and Purification. CopC protein from *P. syringae* was expressed and isolated as described previously.[17] The expression plasmids for wild-type PcoC, nA-PcoC, and other PcoC variants were propagated with *E. coli* DH5α and transformed into BL21(DE3) pLysS for protein expression. A total of 1 L of a 2YT culture containing 100 mg of ampicillin and 34 mg of chloramphenicol was inoculated with 5 mL of an overnight culture of the BL21(DE3) pLysS cells containing each expression plasmid. Cells were grown aerobically with vigorous shaking at 37 °C to OD_{600} ~ 1, and the culture was cooled to room temperature over 1 h before IPTG was added to a final concentration of 0.2 mM to induce protein expression. After 4–5 h of growth at 28 °C, cells were harvested by centrifugation. A clarified lysis extract was prepared in a Tris-Cl buffer (50 mM; pH 8) containing 1 mM EDTA and loaded onto an anion-exchange DE-52 column (3 × 15 cm) to remove negatively charged *E. coli* proteins. The flow-through fraction was adjusted to pH 6 with 0.2 M MES and applied to a CM-52 cation-exchange column. The bound proteins were eluted with a salt gradient of 0–0.3 M NaCl in 20 mM MES. EDTA (1 mM) was included in the CM buffer to ensure removal of contaminating metal ions. *apo*-PcoC proteins were eluted over the

(13) Arnesano, F.; Banci, L.; Bertini, I.; Thompsett, A. R. *Structure* **2002**, *10*, 1337–1347.
(14) Arnesano, F.; Banci, L.; Bertini, I.; Mangani, S.; Thompsett, A. R. *Proc. Natl. Acad. Sci. U.S.A.* **2003**, *100*, 3814–3819.
(15) Arnesano, F.; Banci, L.; Bertini, I.; Felli, I. C.; Luchinat, C.; Thompsett, A. R. *J. Am. Chem. Soc.* **2003**, *125*, 7200–7208.
(16) Koay, M.; Zhang, L.; Yang, B.; Maher, M. J.; Xiao, Z.; Wedd, A. G. *Inorg. Chem.* **2005**, *44*, 5203–5205.
(17) Zhang, L.; Koay, M.; Maher, M. J.; Xiao, Z.; Wedd, A. G. *J. Am. Chem. Soc.* **2006**, *128*, 5834–5850.
(18) Gaggelli, E.; Kozlowski, H.; Valensin, D.; Valensin, G. *Chem. Rev.* **2006**, *106*, 1995–2044.
(19) Sankararamakrishnan, R.; Verma, S.; Kumar, S. *Proteins: Struct., Funct., and Bioinf.* **2004**, *58*, 211–221.
(20) Harford, C.; Sarkar, B. *Acc. Chem. Res.* **1997**, *30*, 123–130.

(21) Wernimont, A. K.; Huffman, D. L.; Finney, L. A.; Demeler, B.; O'Halloran, T. V.; Rosenzweig, A. C. *J. Biol. Inorg. Chem.* **2003**, *8*, 185–194.
(22) Peariso, K.; Huffman, D. L.; Penner-Hahn, J. E.; O'Halloran, T. V. *J. Am. Chem. Soc.* **2003**, *125*, 342–343.
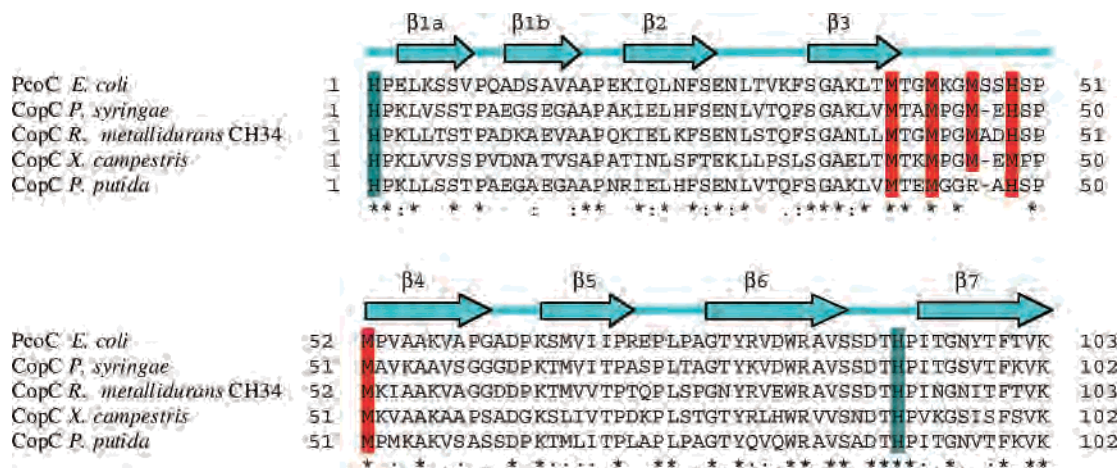
Figure 2. Sequence alignment of plasmid-based copper-resistance homologous *E. coli* PcoC (accession no. s52255), *P. syringae* CopC (accession no. aaa25808) and *R. metallidurans* CH34 CopC (accession no. YP_581923), and chromosomal orthologues *X. campestris* CopC (accession no. c36868) and *P. putida* CopC (accesson no. aap88297). Possible ligands for the Cu^I and Cu^{II} sites of CopC are highlighted in red and teal, respectively. Secondary structure elements as determined from the PcoC crystal structure are shown above the PcoC sequence.

range of 0.10−0.15 M NaCl. The final purification step used a Superdex-75 gel-filtration column (HR16/60; Pharmacia) with eluent 20 mM MES, pH 6, and 100 mM NaCl to remove EDTA and to separate a dimeric component of PcoC (5−10%; see the Supporting Information and Figures S1 and S2). The purity and identity of each isolated protein were confirmed by SDS-PAGE and ESI-MS (Table S2 and Figure S3 in the Supporting Information). Protein yields were about 20 mg per 1 L of culture. The metal content was <0.01 equiv of copper.

Metalated forms of PcoC and its variants were generated as follows: Cu^I forms by the addition of 1.0 mol equiv of $[Cu^I(MeCN)_4]ClO_4$ in MeCN under anaerobic conditions; Cu^{II} forms by the addition of 1.2 mol equiv of $CuSO_4$; Cu^ICu^{II} forms by the addition of 1.2 equiv of $CuSO_4$, followed by 1.2 equiv of $[Cu^I(MeCN)_4]ClO_4$ or by the addition of 2.2 equiv of $CuSO_4$ in the presence of 20 equiv of NH_2OH. In all cases, weakly bound copper ions were removed by gel-filtration or cation-exchange chromatographies.

Concentration Assays. Stock solutions of Cu^I, Cu^{II}, EDTA, and EGTA were standardized according to protocols described previously.[17] Concentrations of bicinchonic acid (bca) solutions used for the Cu^I binding affinity assays were calibrated by titration with a Cu^{II} standard solution in the presence of NH_2OH (20 equiv). Under these conditions, purple $[Cu^I(bca)_2]^{3-}$ with an absorption maximum at 562 nm formed quantitatively until 0.5 equiv of Cu^{II} was added. Concentrations of CopC proteins were estimated from ϵ_{280} values determined previously.[17] PcoC concentrations were also estimated directly from the absorbance at 280 nm. Calculations based on the protein amino acid content estimated $\epsilon_{280} = 8250$ M^{-1} cm^{-1} for *apo*-PcoC. However, quantitative drying of protein samples in the volatile buffer NH_4HCO_3 provided $\epsilon_{280} = 10\ 100$ (±400) M^{-1} cm^{-1}. This value was consistent with that estimated via titration of *apo*-PcoC with a standardized Cu^{II} solution monitored by fluorescence spectroscopy (see parts a and b(i) of Figure 4), assuming that PcoC binds a single 1 equiv of Cu^{II} ion. Consequently, this value was used in this work. The concentrations of metalated species were estimated by the Bradford method using *apo*-PcoC as the standard. The derived molar absorptivities ϵ_{280} were 11 500, 12 100, and 14 300 M^{-1} cm^{-1} for the Cu^I, Cu^{II}, and Cu^ICu^{II} forms, respectively.

The copper content in each isolated protein sample was determined spectrophotometrically by the reaction with at least 20 equiv of Cu^I-specific colorimetric reagent bathocuproine disulfonate

Table 1. Analytical Data for Components Eluted from a Mono-S Cation-Exchange Column (Figure 3) and a Gel-Filtration Column (Figure S1 in the Supporting Information)[a]

entry	figure	concn of NaCl (mM)[b]	molar mass (Da)[c]	Cu^I-PcoC	Cu^{II}-PcoC	assignment
1	3a	~90	10 979	nd[d]	nd	wt □□
2	3b	~100	10 979	nd	1.0	wt □Cu^{II}
3	3c	~112	10 979	1.0	1.0	wt Cu^ICu^{II}
4	S1		11 050	nd	0.9₅	Cu^{II}-nA-PcoC
5	S1		11 050	1.0	nd	Cu^I-nA-PcoC
6	S1		11 050	1.0	1.0	Cu^ICu^{II}-nA-PcoC
7	3d	~87	10 989	nd	nd	H1F □X
8	3e	~100	10 989	0.9	nd	H1F Cu^IX
9	3f	~82	10 971	nd	nd	*apo*-M40L/H49F
10	3g	~91	10 971	nd	1.0	Cu^{II}-M40L/H49F

[a] Protein concentrations were estimated by A_{280} using ϵ_{280} values of 11 500, 12 100, and 14 300 M^{-1} cm^{-1} for Cu^I, Cu^{II}, and Cu^ICu^{II} forms, respectively. Cu^I and Cu^{II} concentrations were estimated spectrophotometrically by reagent bcs as detailed in the Experimental Section. [b] Observed elution concentrations depended on the protein concentration, ionic strength, and sample volume so some variation was observed from experiment to experiment. [c] Determined as the *apo* form by ESI-MS in an acidic solvent. [d] Not detected.

(bcs).[23] The Cu^I content was determined directly without the addition of a reductant. The total copper content (and, hence, the Cu^{II} content by difference) was estimated by the subsequent addition of reductant NH_2OH to the same solution. Results are given in Table 1.

Protein Characterization. The effective separation of *apo*-PcoC and various metalated forms was achieved via NaCl gradient elution on a Mono-S cation-exchange column (HR5/5; Pharmacia) in KPi (10 mM; pH 7). The identity of each eluted protein component was established by ESI-MS analysis under acidic conditions, while its Cu^I and Cu^{II} contents were estimated by copper analysis (see Table 1).

The aggregation states of both *apo* and metalated forms of PcoC in solution were analyzed via elution on a Superdex-75 gel-filtration column (HR10/30; Pharmacia) at a flow rate of 0.7 mL min^{-1} in a KPi buffer (20 mM; pH 7) and NaCl (100 mM) (Figure S1 in the Supporting Information). Spectroscopic characterization and ESI-MS were carried out as described previously.[17]

(23) Blair, D.; Diehl, H. *Talanta* **1961**, 7, 163−174.

Oxidation of Cu^I Proteins and Reduction of Cu^{II} Proteins. The unique tryptophan Trp84 in *apo*-PcoC fluoresced intensely at $\lambda_{max} = 325$ nm when excited at 290 nm (see Figure 4). Cu^{II} binding quenched the fluorescence intensity linearly until 1 equiv of Cu^{II} was bound, but Cu^I binding had no effect. Reduction or removal of the bound Cu^{II} led to quantitative restoration of the fluorescence intensity. Consequently, oxidation and reduction processes could be monitored.

To monitor oxidation of the Cu^I form, an *apo*-protein solution ($5-10$ μM) was prepared anaerobically in a KPi buffer (20 mM; 100 mM NaCl, pH 7) in a glovebox ($O_2 < 10$ ppm) and loaded into a fluorescence cell sealed with a septum cap. After the fluorescence intensity was recorded at 325 nm (F_0), 1 equiv of $[Cu^I(MeCN)_4]^+$ in MeCN was injected from an airtight syringe. To initiate oxidation, the septum cap of the cuvette was removed to admit air. It was replaced immediately and the cuvette inverted several times to mix the solution and atmosphere. The dioxygen concentration in an air-saturated aqueous solution is estimated to be $\sim$270 μM,[24] and the above process was sufficient to induce a steady oxidation of the Cu^I proteins at a concentration of $5-10$ μM used in the present experiments (see Figure 7).

Oxidation was monitored via changes in the fluorescence intensity with time. The results were expressed as the binding site occupancy for Cu^{II}, $\Delta F_x / \Delta F_1 = (F_0 - F_x)/(F_0 - F_1)$. F_0, F_x, and F_1 are the fluorescence intensities when the Cu^{II} binding site is occupied by 0, x, and 1 equiv of Cu^{II}, respectively.

To monitor reduction of the Cu^{II} forms, each protein sample ($5-10$ μM) was prepared anaerobically in a fluorescence cell sealed with a septum cap in a glovebox. Reduction was initialized by the injection of either NH_2OH (20 equiv) or sodium ascorbate (asc; 3 equiv) and the reduction process monitored via changes in the fluorescence intensity with time. The results also were expressed as binding site occupancies for Cu^{II} (see above). F_0 was estimated by the addition of 50 equiv of EDTA into the protein solution to convert all protein forms into the *apo* form. When NH_2OH was used as a reductant, F_1 was the fluorescence intensity before reduction. When asc was used as a reductant, F_1 could not be read directly from the experiment because asc absorbs strongly at the excitation wavelength of $\sim$280 nm. However, F_1/F_0 was found to have constant values of 0.32(2), 0.46(2), and 0.52(2) for CopC, PcoC, and nA-PcoC, respectively. Consequently, the F_1 values could be estimated from the respective F_0 values.

The oxidation and reduction products were analyzed selectively for wild-type PcoC proteins by elution on a Mono-S cation-exchange column with a deoxygenated KPi buffer (10 mM; pH 7).

Estimation of Metal Dissociation Constants. Cu^I Dissociation Constants. We have previously developed an approach for estimation of the affinity of proteins for Cu^I based on competition with ligand bcs (Figure S4 in the Supporting Information).[25] The same approach was adapted here for estimation of the Cu^I affinity of PcoC but with a weaker Cu^I ligand bca (Figure S4 in the Supporting Information) to ensure effective competition (P = PcoC or CopC):

$$apo\text{-}P + [Cu^I(bca)_2]^{3-} \rightleftharpoons Cu^I\text{-}P + 2bca^{2-} \qquad K_{ex} \quad (1)$$
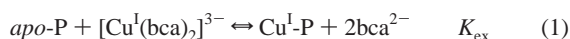
When bca is in excess, a single stable 1:2 purple complex $[Cu(bca)_2]^{3-}$ is present that features absorption maxima at 562 nm ($\epsilon = 7900$ M^{-1} cm^{-1}) and 358 nm ($\epsilon = 42\,900$ M^{-1} cm^{-1}), respectively.[26] While both the *apo*-P and Cu^I-P proteins do not

absorb at these wavelengths, UV absorption from bca occurs at $\lambda \leq 370$ nm. Consequently, quantitative assays using the band at 358 nm required a background reference solution of bca at the same concentration as that of the sample solution. The association constant $\beta_2 = K_1K_2$ of $[Cu(bca)_2]^{3-}$ is not known, but a reliable comparison of the relative $K_D(Cu^I$-P$)$ values of the PcoC and CopC proteins can be made via eq 2,

$$K_D(Cu^I\text{-}P) = (1/\beta_2)(K_{ex})^{-1} = (1/\beta_2)\frac{[Cu^I(bca)_2][P]}{[Cu^I\text{-}P][bca]^2} \quad (2)$$

where K_{ex} is the equilibrium constant for exchange reaction 1.

With known total concentrations of Cu^I, bca, and protein, the equilibrium concentration of each species in eq 1 can be obtained from the observed equilibrium concentration of $[Cu^I(bca)_2]^{3-}$, and thus the dissociation constant $K_D(Cu^I$-P$)$ relative to β_2 can be estimated from eq 2 and compared for different proteins.

Experiments were conducted under anaerobic conditions as described previously.[25] Briefly, varying amounts of *apo*-proteins were added to a solution containing $[Cu^I(bca)_2]^{3-}$ prepared by mixing $[Cu^I(MeCN)_4]ClO_4$ and bca in a molar ratio of 1:2.5 (to ensure the presence of the 1:2 complex). The mixtures were diluted to the same total concentrations of Cu^I and bca but different total concentrations of proteins. asc (100 μM final concentration) was added to maintain the Cu^I oxidation state. Equilibration was attained after incubation for 20 min, and the transfer of Cu^I from bca to protein was estimated by the change in absorbance at 358 nm (or at 562 nm but with decreased sensitivity) relative to a control solution without protein. Competition was evident from a stepwise decrease in absorptions at both 358 and 562 nm upon a stepwise increase in the total protein concentration under anaerobic conditions (see Figure S5 in the Supporting Information).

Cu^{II} Dissociation Constants. The affinity of PcoC proteins for Cu^{II} was estimated by competition with the Cu^{II} ligand EGTA according to reaction 3

$$apo\text{-}PcoC + Cu^{II}(EGTA) \rightleftharpoons Cu^{II}\text{-}PcoC + EGTA \quad (3)$$
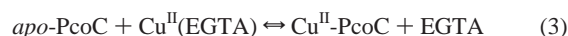
and the associated relationship 4 under the conditions of effective competition of eq 3,

$$K_DK_A = \left(\frac{[PcoC]_{total}}{[Cu^{II}\text{-}PcoC]} - 1\right)\left(\frac{[EGTA]_{total}}{[Cu^{II}(EGTA)]} - 1\right) \quad (4)$$

where K_D is the dissociation constant of Cu^{II}-PcoC and K_A is the apparent association constant of $Cu^{II}(EGTA)$ under the experimental conditions.[27] Experimental details and the derivation of eq 4 have been given previously.[17]

Results and Discussion

Characterization of the nA-PcoC Protein. The design used previously to facilitate cloning of the *E. coli pcoC* gene without the leader sequence led to expression and isolation of a form of the PcoC protein featuring Ala as the N-terminal residue, demoting the native His1 to position 2 (Figure 2).[11] This form is designated here as nA-PcoC and bound 1 equiv of either Cu^I or Cu^{II} in solution. It was converted quantitatively to an air-stable Cu^I form upon reduction with asc.

(24) Atkins, P.; de Paula, J. *Physical Chemistry*, 7th ed.; Freeman: New York, 2001; p 172.
(25) Xiao, Z.; Loughlin, F.; George, G. N.; Howlett, G. J.; Wedd, A. G. *J. Am. Chem. Soc.* **2004**, *126*, 3081−3090.
(26) Xiao, Z.; Wedd, A. G., unpublished observations.
(27) Martell, A. E., Smith, R. M., Eds. *Critical Stability Constants, Vol. 1: Amino Acids*; Plenum: New York, 1974.

Physical characterization was consistent with the presence of $Cu^I(His)(Met)_2$ and $Cu^{II}(His)_2(N/O)_2$ centers.[11,22]

PcoC from *E. coli* is a homologue of CopC from *P. syringae*, sharing 67% sequence identity (Figure 2).[17,21] CopC also features two distinct copper binding sites specific for Cu^I and Cu^{II}.[14,17] Reaction with asc or dithionite converted its stable Cu^{II} form to the Cu^I form, which, in contrast to air-stable Cu^I-nA-PcoC, was highly air-sensitive and oxidized rapidly to the Cu^{II} form. However, the bound Cu^I was stable in air if the Cu^{II} site in CopC was occupied or disabled. We were prompted to re-examine the copper binding properties of nA-PcoC and to generate its wild-type form for comparison with CopC.

Generation and Characterization of Wild-Type PcoC and Variant Forms. To express PcoC protein in its wild-type form, an expression plasmid pDX905 was constructed that incorporated a chimeric gene encoding the CopC leader sequence followed by the PcoC protein sequence. The leader sequence was processed correctly by the *E. coli* expression host, and the isolated protein was confirmed by ESI-MS to be the mature form of the native PcoC protein without the leader peptide (Table S2 and Figure S3 in the Supporting Information). An indistinguishable native PcoC protein was isolated from the equivalent expression of a full-length *pcoC* gene encoding both the leader and protein sequences isolated from the *pco* operon. To assist in the definition of copper binding sites, several protein variants were generated and their identities confirmed by ESI-MS (Tables S1 and S2 in the Supporting Information).

Three copper-loaded forms of Cu^I-, Cu^{II}-, and Cu^ICu^{II}-PcoC were generated by the addition of 1 equiv of Cu^I and/or Cu^{II} to *apo*-PcoC, demonstrating that, like CopC, PcoC possessed two distinct copper sites: one is specific for Cu^I and the other for Cu^{II}. Available structural data indicate that the two copper binding sites in PcoC are located at the ends of the β-barrel molecule and separated by ~30 Å.[17,21] For efficient notation, an empty copper site in wild-type PcoC or CopC is indicated by $\square$. Hence, the *apo* forms are $\square\square$, the half-loaded forms are $Cu^I\square$ and $\square Cu^{II}$, and the fully loaded forms are Cu^ICu^{II}. The $\square Cu^{II}$ and Cu^ICu^{II} forms were stable in air and could be isolated in substance via cation-exchange chromatography (Figures 3a–c and Table 1, entries 1–3).

Wild-type PcoC differs from nA-PcoC in three aspects: (i) Cu^{II}-PcoC ($\square Cu^{II}$) is blue ($\lambda_{max} = 610$ nm; $\epsilon = 110$ M^{-1} cm^{-1}) at pH 7, while Cu^{II}-nA-PcoC is purple ($\lambda_{max} = 576$ nm; Figure S6 in the Supporting Information); (ii) the affinity of PcoC for Cu^{II} is increased dramatically over that of nA-PcoC (see ligand competition experiments detailed later; notation $\square\Downarrow$ is used for *apo*-nA-PcoC to indicate the lower affinity for Cu^{II}); (iii) Cu^I-PcoC ($Cu^I\square$) was oxidized by dioxygen to $\square Cu^{II}$ quantitatively in about 1 h upon exposure to air (see Figure 7Ib), while, in sharp contrast, Cu^I-nA-PcoC ($Cu^I\Downarrow$) is air-stable.

Differences in (i) and (ii) clearly indicate an alteration in the Cu^{II} binding site upon removal of the N-terminal residue Ala in nA-PcoC and are consistent with His1 as a bidentate ligand for Cu^{II} in the wild-type PcoC, as observed in an X-ray
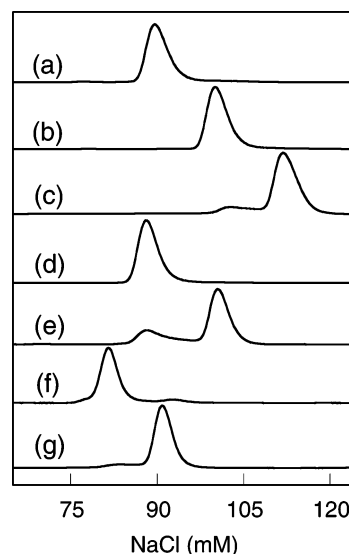

Figure 3. Elution profiles of PcoC proteins (~100 μg) on a Mono-S HR5/5 cation-exchange column (0.5×5 cm) in a buffer (10 mM KPi; pH 7.0; NaCl gradient 0–200 mM). Protein identities were confirmed by protein and metal analysis (see Table 1): (a) *apo*-PcoC $\square\square$; (b) wild-type $\square Cu^{II}$, formed upon mixing $\square\square$ (1 equiv) and $CuSO_4$ (>1 equiv); (c) wild-type Cu^ICu^{II}, formed upon mixing $\square\square$ (1 equiv), $CuSO_4$ (>2 equiv), and NH_2-OH (20 equiv) (the increased absorbance starting at the elution position of $\square Cu^{II}$ is due to slow oxidation of Cu^ICu^{II} by air promoted by the affinity of the Mono-S resin for Cu^{II} ions (cf. eq 9); (d) H1F $\square X$ alone or a mixture of $\square X$ (1 equiv) and $CuSO_4$ (>1 equiv); (e) H1F Cu^IX, formed upon mixing $\square X$ (1 equiv), $CuSO_4$ (1.2 equiv), and NH_2OH (20 equiv) (the increased absorbance starting at the elution position of $\square X$ is due to slow oxidation of Cu^IX by air promoted by the affinity of the Mono-S resin for Cu^{II} ions (cf. eq 9); (f) *apo*-H40M/H49F $\Downarrow\square$; (g) $\Downarrow Cu^{II}$, formed upon mixing $\Downarrow\square$ (1 equiv) and $CuSO_4$ (>1 equiv) with or without NH_2OH.

structure of the CopC protein.[17] The difference in (iii) can also be attributed to the presence of a high-affinity Cu^{II} binding site in PcoC but not in nA-PcoC: the relative affinities of the Cu^I and Cu^{II} sites in PcoC are such that the oxidation of $Cu^I\square$ by dioxygen via intermolecular transfer of Cu^{II} is thermodynamically favorable for that protein but not for $Cu^I\Downarrow$. Consequently, $Cu^I\Downarrow$ is stable in air and can be isolated in pure form via gel filtration (Table 1, entry 5, and Figure S1 in the Supporting Information). Subsequent addition of Cu^{II} to $Cu^I\Downarrow$ generated the Cu^ICu^{II} form that also survived gel filtration (Table 1, entry 6, and Figure S1 in the Supporting Information).

Mutation of the Cu^{II} ligand His1 to Phe produced the PcoC variant protein H1F, whose *apo* form is designated as $\square X$. The Cu^{II} binding site is essentially disabled because the benzyl side chain cannot act as a ligand and its steric requirements may interfere with the amino terminus acting as a ligand. Its Cu^{II} form did not survive cation-exchange chromatography (Figure 3d) and could not be detected spectroscopically upon the addition of excess Cu^{II} to a 50 μM solution of $\square X$. However, because of the lower Cu^{II} affinity, the Cu^I form Cu^IX was air-stable and could compete with the cation-exchange resin for copper (Figure 3e and Table 1, entry 8).

Mutation of the Cu^{II} ligand His92 to Phe produced the variant H92F, which also exhibited weakened Cu^{II} binding and is consequently denoted by $\square\downarrow$. Its $Cu^I\downarrow$ form remained air-sensitive (see Figure 7Ic). Presumably, the presence of

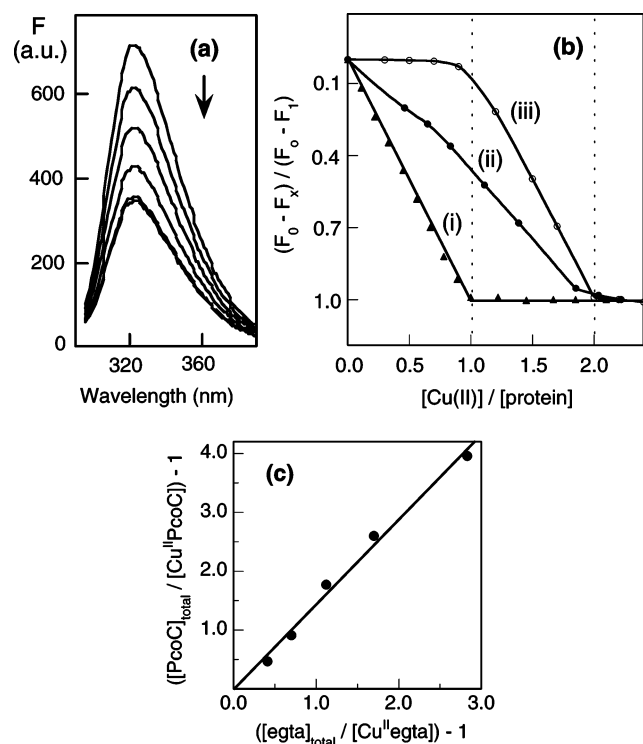**Figure 4.** Determination of Cu^{II} dissociation constants $K_D(\square Cu^{II})$ for PcoC proteins (5 μM) in a KPi buffer (20 mM; pH 7.0; NaCl, 100 mM): (a) quenching of the fluorescence emission intensity for *apo*-PcoC $\square\square$ upon titration with a Cu^{II} solution (100 μM); (b) change in the fluorescence emission intensity (expressed as the Cu^{II} occupancy) as a function of the Cu^{II} concentration in the presence of (i) wild-type PcoC ($\square\square$) in a KPi buffer only, (ii) $\square\square$ (or $\downarrow\square$) and EGTA (5.0 μM), and (iii) $\square\downarrow$ (or $\square\Downarrow$) and EGTA (5.0 μM); (c) plot of eq 4 (Table S3 in the Supporting Information) for effective competition for Cu^{II} between $\square\square$ and EGTA.

bidentate His1 ensures that the affinity of the site for Cu^{II} is sufficient to make the oxidation to Cu^{II} thermodynamically viable.

Mutation of the potential Cu^{I} ligands Met40 to Leu and/or His49 to Phe generated three protein variants, M40L, H49F, and M40L/H49F, whose *apo* forms are denoted by $\downarrow\square$. Their $Cu^{I}Cu^{II}$ forms did not survive the cation-exchange column (Figure 3f,g and Table 1, entries 9 and 10), confirming a lower affinity for Cu^{I} and the involvement of both M40 and H49 in Cu^{I} binding in these protein variants at pH 7.

All forms of isolable PcoC proteins (e.g., $\square\square$, $\square Cu^{II}$, $Cu^{I}Cu^{II}$, $Cu^{I}\Downarrow$, $Cu^{I}X$, and $\downarrow Cu^{II}$; see Table 1) eluted indistinguishably from the analytical gel-filtration column at pH 7. The elution volumes were consistent with monomeric protein molecules in solution (see Figure S1 in the Supporting Information).

Cu^{II} Dissociation Constant and Intermolecular Cu^{II} Transfer. The unique tryptophan Trp84 located between the two copper binding sites fluoresced intensely at λ_{max} = 325 nm when excited at 290 nm (Figure 4a), allowing Cu^{II} binding to be monitored quantitatively. The addition of Cu^{II} to the wild-type *apo*-PcoC protein ($\square\square$; 5 μM) quenched the fluorescence intensity linearly until 1 equiv was bound (Figure 4a,b(i)). Conversely, removal of bound Cu^{II} restored the fluorescence intensity completely.
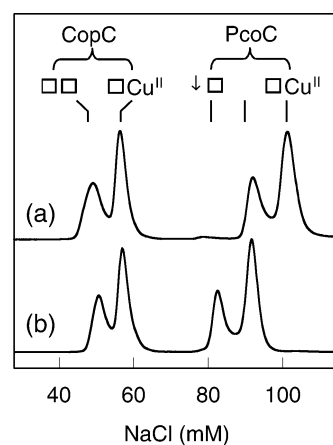

Figure 5. Elution profiles of CopC and PcoC product proteins under the conditions of Figure 3. Protein identities were confirmed by ESI-MS and copper content analysis: (a) reaction of *either apo*-CopC ($\square\square$) and Cu^{II}-PcoC ($\square Cu^{II}$) *or* Cu^{II}-CopC ($\square Cu^{II}$) and *apo*-PcoC ($\square\square$); (b) reaction of *either apo*-CopC ($\square\square$) and Cu^{II}-M40L/H49F-PcoC ($\downarrow Cu^{II}$) *or* Cu^{II}-CopC ($\square Cu^{II}$) and *apo*-M40L/H49F-PcoC ($\downarrow\square$).
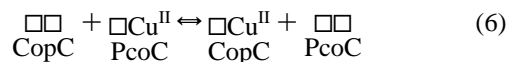
The sharp end point observed in Figure 4b(i) for a protein concentration of 5 μM confirms that the dissociation constant $K_D(Cu^{II}$-P$)$ is $<10^{-6}$ M for wild-type PcoC. However, the same titration with H1F-PcoC ($\square X$) at 10× concentration (50 μM) exhibited little change in the fluorescence intensity and no turning point, suggesting that $K_D(Cu^{II}$-P$) > 10^{-5}$ M for this protein, i.e., that the Cu^{II} site is disabled. This behavior is consistent with the key role of His1 in PcoC in binding Cu^{II} as a bidentate chelating ligand, as is the case for CopC.

In the presence of 1 equiv of the Cu^{II} ligand EGTA, equivalent experiments at pH 7 produced the titration curves shown in Figure 4b(ii) for $\square\square$ and in Figure 4b(iii) for $\square\Downarrow$ and $\square\downarrow$. $\square\square$ competed effectively with EGTA for Cu^{II}, but $\square\Downarrow$ and $\square\downarrow$ did not. For experimental conditions where the Cu^{II} occupancy on both $\square\square$ and EGTA varied between 0.1 and 0.9, a plot of eq 4 produced a straight line passing through the origin (Figure 4c). The slope, plus the known association constant $K_A[Cu^{II}(EGTA)]$,[27] provided a reliable estimation of $K_D(Cu^{II}$-P$)$ of $6(1) \times 10^{-14}$ M for wild-type PcoC (Table S3 in the Supporting Information).

Similar experiments provided the order of $K_D(Cu^{II}$-P$)$ (decreasing affinity) for PcoC proteins given in eq 5.

$$10^{-15} < \square\square = \downarrow\square \sim 10^{-13} < \square\downarrow < \square\Downarrow < 10^{-6} < \square X \quad (5)$$

Incubation of equimolar solutions of wild-type CopC and wild-type PcoC with a single 1 mol equiv of Cu^{II} prebound to either molecule led to essentially equimolar distribution of copper over the two molecules (Figure 5), confirming that their affinities for Cu^{II} are very similar.

$$\underset{\text{CopC}}{\square\square} + \underset{\text{PcoC}}{\square Cu^{II}} \rightleftharpoons \underset{\text{CopC}}{\square Cu^{II}} + \underset{\text{PcoC}}{\square\square} \quad (6)$$

This is an intermolecular Cu^{II} transfer reaction without a change in the oxidation state.

Cu^{I} Dissociation Constant and Intermolecular Cu^{I} Transfer. The ligand bca (Figure S4 in the Supporting
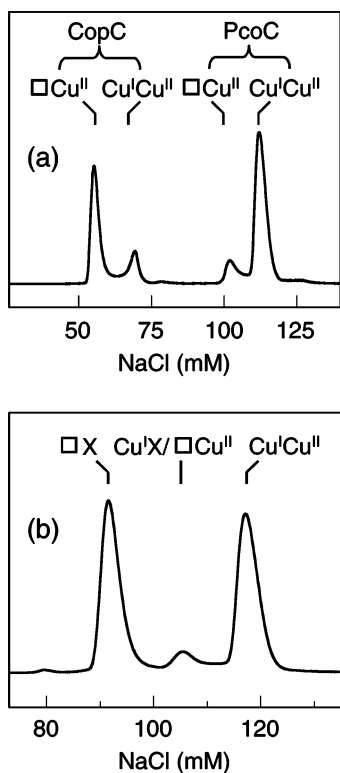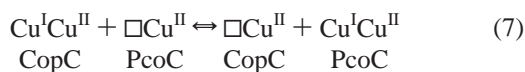
Figure 6. Elution profiles of CopC and PcoC product proteins on a Mono-S HR5/5 cation-exchange column under the conditions of Figure 3. Protein identities were confirmed by ESI-MS and elemental analysis for Cu^I and Cu^{II}: (a) reaction of *either* Cu^{II}-CopC ($\square Cu^{II}$) and $Cu^I Cu^{II}$-PcoC ($Cu^I Cu^{II}$) *or* $Cu^I Cu^{II}$-CopC ($Cu^I Cu^{II}$) and Cu^{II}-PcoC ($\square Cu^{II}$); (b) reaction of the PcoC proteins $Cu^I X$ (H1F) and wild-type $\square Cu^{II}$.

Information) forms a stable 1:2 purple complex $[Cu^I(bca)_2]^{3-}$ and was able to compete with the proteins for Cu^I (Figure S5 in the Supporting Information).[26] Although the association constant β_2 for bca is not known, it was possible to assess the relative affinities of the different proteins for Cu^I via estimation of ratios $K_D(Cu^I\square)/\beta_2$ via eq 2. Full details and numerical data are listed in Table S4 in the Supporting Information.

The derived ratio $K_D(Cu^I\text{-CopC})/K_D(Cu^I\text{-PcoC})$ is ~2, implying that PcoC has a slightly higher affinity for Cu^I. This conclusion is consistent with the observation that incubation of equimolar solutions of Cu^{II}-CopC and Cu^{II}-PcoC with a single 1 mol equiv of Cu^I prebound to either molecule led to ~80% of the Cu^I bound to PcoC and ~20% bound to CopC (Figure 6a).

$$Cu^I Cu^{II} + \square Cu^{II} \Leftrightarrow \square Cu^{II} + Cu^I Cu^{II} \qquad (7)$$
$$\text{CopC} \quad \text{PcoC} \quad \text{CopC} \quad \text{PcoC}$$

The Cu^I transfer reaction 7 was carried out in air, which underlines the fact that an empty high-affinity Cu^{II} site is essential for the oxidation of Cu^I in these systems. This aspect is further emphasized by the reaction of the PcoC proteins $Cu^I X$ (with its disabled Cu^{II} site) and wild-type $\square Cu^{II}$ (with its blocked Cu^{II} site) (Figure 6b).

$$Cu^I X + \square Cu^{II} \rightarrow \square X + Cu^I Cu^{II} \qquad (8)$$
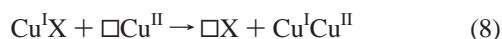
Reactions 7 and 8 are both intermolecular Cu^I transfer reactions without a change in the oxidation state. However,
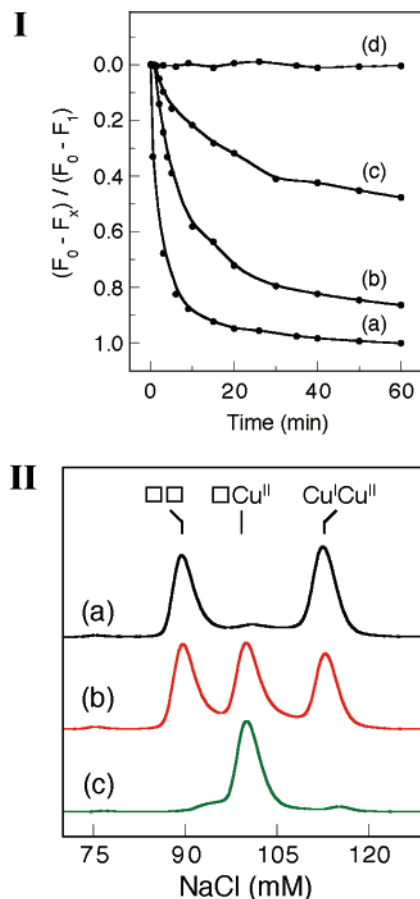
Figure 7. (I) Time course of a change in the fluorescence emission intensity at 325 nm of Cu^I proteins (5.0 μM; KPi, 20 mM, pH 7) upon introduction of air. Results are expressed as the Cu^{II} site occupancy $\{(F_0 - F_x)/(F_0 - F_1)\}$: (a) Cu^I-CopC ($Cu^I\square$); (b) Cu^I-PcoC ($Cu^I\square$); (c) H92F Cu^I-PcoC ($Cu^I\Downarrow$); (d) Cu^I-nA-PcoC ($Cu^I\square\Downarrow$) or Cu^I-H1F PcoC ($Cu^I X$). (II) Oxidation of wild-type PcoC protein $Cu^I\square$ by air. Elution profiles of product proteins on a Mono-S HR5/5 cation-exchange column under the conditions of Figure 3. The sample was injected (a) immediately after preparation (see text), (b) after exposure to air for 2 min, and (c) after exposure to air for 80 min. The intense peaks in parts a−c have been normalized for clarity of presentation. Figure S7 in the Supporting Information is equivalent with the experimentally observed relative intensities.

the source of the driving force for reaction 8 is intriguing, and the same phenomenon was observed in the CopC system.[17] Within experimental error, the affinity of $\square X$ for Cu^I is indistinguishable from that of $\square\square$ (Table S4 in the Supporting Information). Consequently, occupation of the Cu^{II} site of $\square\square$ to form $\square Cu^{II}$ appears to have increased the affinity for Cu^I at its site, ~30 Å away. This aspect is addressed further below.

Two-Step Intermolecular Copper Transfer. Oxidation of the Cu^I Protein. Oxidation was induced by introduction of excess dioxygen into solutions of the wild-type PcoC and CopC forms $Cu^I\square$ and was followed by fluorescence spectroscopy (Figure 7Ia,b). The $Cu^I\square$ forms were oxidized cleanly.

$$Cu^I\square \xrightarrow{O_2} \square Cu^{II} \qquad (9)$$

The relative rates of oxidation were reproducible: $t_{1/2} \sim 2$ and 10 min for CopC and PcoC, respectively. The order

correlates with the higher affinity of PcoC for Cu^I (Figure 6a and Table S4 in the Supporting Information). The relative slowness of this oxidation in the PcoC system has allowed unequivocal detection of reaction intermediates (see below), *which was not possible in the CopC system.*[17]

The rates of oxidation decreased in the order Cu$^I\square$ > Cu$^I\Downarrow$ > Cu$^I\Downarrow$ > Cu^{I}X (Figure 7Ib–d), which is the order of decreasing affinity for Cu^{II} (eq 5). In fact, both Cu^{I}X and Cu$^I\Downarrow$ were air-stable, but Cu^{I}X survived oxidative competition with the MonoS cation-exchange resin (Figure 3e) while Cu$^I\Downarrow$ did not. It is apparent that the rate of oxidation reaction 9 depends upon the relative affinities of *both* binding sites.

The course of the oxidation was also followed by cation-exchange chromatography. When an anaerobic sample of Cu$^I\square$ was injected into the column equilibrated in a deoxygenated buffer, followed by immediate commencement of the NaCl gradient, limited reaction with air occurred before separation of the products. Equimolar concentrations of air-stable products $\square\square$ and Cu^{I}Cu^{II} were detected (Figure 7IIa).

$$2Cu^I\square \xrightarrow{O_2} \square\square + Cu^ICu^{II} \qquad (10)$$

Reaction 10 is driven by the presence of an empty high-affinity Cu^{II} site on each of the Cu$^I\square$ molecules. Significantly, little $\square$Cu^{II} was evident from the elution profile (Figure 7IIa), consistent with intermolecular rather than intramolecular transfer of copper.

Longer exposure of Cu$^I\square$ to air led to increasing concentrations of the final product $\square$Cu^{II} at the expense of intermediates $\square\square$ and Cu^{I}Cu^{II} (Figure 7IIb,c).

$$\square\square + Cu^ICu^{II} \xrightarrow{O_2} 2\square Cu^{II} \qquad (11)$$

Reaction 11 is again driven by the presence of an empty high-affinity Cu^{II} site on the $\square\square$ molecules. It is apparent that reaction 9 consists of two steps: reaction 10 is followed by reaction 11, but reaction 10 is completed before reaction 11 proceeds (Figure 7IIa). These relative rates can be rationalized by the same explanation offered above for the thermodynamic viability of reaction 8: occupation of the Cu^{II} site has increased the affinity for Cu^I at its site, ~30 Å away.

The *apo* protein $\square\square$ is one of the products of reaction 10 and so could also act as a reactant to accept Cu^{II}, providing an alternative reaction pathway.

$$Cu^I\square + \square\square \xrightarrow{O_2} \square\square + \square Cu^{II} \qquad (12)$$

However, low concentrations only of $\square$Cu^{II} were detected in the first copper transfer reaction (Figure 7IIa). Under the reaction conditions, this result may be interpreted in two ways: (i) reaction 12 was significantly slower than reaction 10 or (ii) Cu^I and/or Cu^{II} transfer occurred rapidly between the two half-loaded species Cu$^I\square$ and $\square$Cu^{II}, and the latter species $\square$Cu^{II} formed transiently in the presence of an excess of Cu$^I\square$. A plausible rationalization lies with a complementary argument to that proposed for reaction 8 and the fact that reaction 10 is faster than reaction 11: occupation of
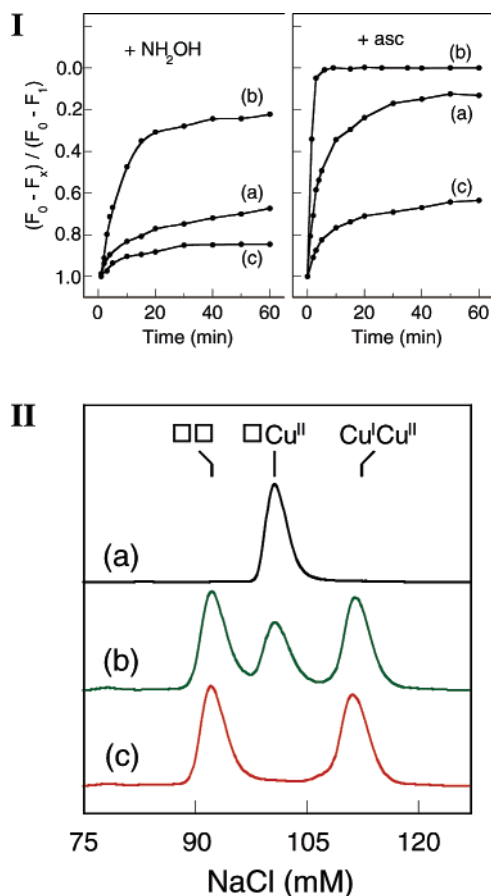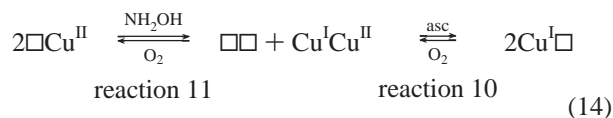

Figure 8. (I) Time course of a change in the fluorescence emission intensity at 325 nm of Cu^{II}-CopC proteins (5.0 μM; KPi, 20 mM, pH 7) upon reduction with NH$_2$OH (20 equiv; left panel) or asc (3 equiv; right panel). Results are expressed as the Cu^{II} site occupancy $\{(F_0 - F_x)/(F_0 - F_1)\}$: (a) Cu^{II}-PcoC; (b) Cu^{II}-nA-PcoC; (c) Cu^{II}-M40L/H49F PcoC ($\downarrow$Cu^{II}). (II) Reduction of wild-type PcoC protein $\square$Cu^{II} under anaerobic conditions. Elution profiles of product proteins on a Mono-S HR5/5 cation-exchange column under the conditions of Figure 3: (a) no reductant; (b) reaction with NH$_2$OH (20 equiv) for 1 h; (c) reaction with asc (3 equiv) for 1 h. The peaks in parts a–c have been normalized for clarity of presentation.

the Cu^I site appears to have increased the affinity for Cu^{II} at its site, ~30 Å away.

Two-Step Intermolecular Copper Transfer. Reduction of the Cu^{II} Protein. Reduction of the wild-type PcoC protein $\square$Cu^{II} induced migration of the copper ion from the Cu^{II} site to the Cu^I site.

$$Cu^{II} \xrightarrow{+e^-} Cu^I\square \qquad (13)$$

Anaerobic reduction by the weaker reductant NH$_2$OH (20 equiv) and by the stronger reductant asc (3 equiv) was followed by fluorescence spectroscopy (Figure 8Ia). The initial rate of reduction is higher for asc, and the reaction was complete after 1 h. The products were analyzed by cation-exchange chromatography in air. After separation, three air-stable protein species, $\square\square$, $\square$Cu^{II}, and Cu^{I}Cu^{II}, were detected in the NH$_2$OH reaction after 1 h (Figure 8IIb), but only $\square\square$ and Cu^{I}Cu^{II} were present with asc (Figure 8IIc). The results are consistent with a two-step reduction process for reaction 13 in which $\square$Cu^{II} acts effectively as a catalyst for the oxidation of NH$_2$OH and asc by dioxygen:

$$2\square Cu^{II} \underset{O_2}{\overset{NH_2OH}{\rightleftharpoons}} \square\square + Cu^ICu^{II} \underset{O_2}{\overset{asc}{\rightleftharpoons}} 2Cu^I\square$$

reaction 11   reaction 10

         (14)

The faster rate of reduction by asc led to quantitative formation of $Cu^I\square$, followed by its subsequent oxidation on the chromatographic column via reaction 10, leading to equimolar yields of $\square\square$ and Cu^ICu^{II} (Figure 8IIc). This underscores the previous conclusion that reaction 10 is faster than reaction 11.

The initial rate of reduction and the final equilibrium position depended on both the strength of the reductant and the relative affinities of the Cu^I and Cu^{II} sites. The rate was faster for the Cu^{II} form of nA-PcoC ($\square\Downarrow$) than for the Cu^{II} form of wild-type PcoC ($\square\square$; Figure 8Ia,b) but slower for the Cu^{II} form of M40L/H49F-PcoC ($\Downarrow\square$; Figure 8Ia,c). The weaker reductant NH_2OH reduced all of the Cu^{II} proteins more slowly than did the stronger reductant asc under the same conditions. However, neither NH_2OH nor asc was able to reduce bound Cu^{II} in wild-type Cu^ICu^{II}-PcoC because the Cu^I site is filled.

Summary

The role of the His1 residue in Cu^{II} binding is confirmed for both the PcoC and CopC proteins. It acts effectively as a bidentate ligand, with both the imidazole ring and the N terminus being bound as part of the Cu^{II}(His1)(His92) (N-term)(OH_x) center (Figure 1c). The addition of an extra Ala residue in the N terminus in PcoC demoted His1 to position 2 and weakened Cu^{II} binding to such an extent that the Cu^I form became stable in air and was unable to participate in oxidative intermolecular transfer of copper as Cu^{II} (eq 9). Mutation of His1 to Phe disabled the Cu^{II} site completely.

The observation of discrete intermediates in both the oxidative and reductive transfer of copper (eqs 9–11, 13, and 14) in PcoC confirmed unequivocally that the mechanism of copper transfer is intermolecular rather than intramolecular.

Modulation of metal affinities via changes of available ligands in variant forms of PcoC and CopC demonstrated that high-affinity empty sites must be available to receive the transferring ion. Thus, the decreasing Cu^{II} binding affinity in the series $\square\square > \square\Downarrow > \square\Downarrow > \square X$ was accompanied by a complementary increase in the redox stability of the Cu^I forms (Figure 7I). On the other hand, a decrease in the Cu^I affinity in $\Downarrow\square$ was associated with an increase in the redox stability for the Cu^{II} form $\Downarrow Cu^{II}$ (Figure 8I).

There is evidence for a more subtle modulation of metal affinities associated with occupation of the individual Cu^I and Cu^{II} sites, separated by ~30 Å:

(1) Occupation of the Cu^{II} site in $\square\square$ increases the affinity for Cu^I at its site, rationalizing the viability of reaction 8 and the fact that reaction 11 is slower than reaction 10.

(2) Occupation of the Cu^I site in $\square\square$ increases the affinity for Cu^{II} at its site, rationalizing the fact that reaction 12 is slower than reaction 10.

While the resolution of present NMR and X-ray crystallographic data is insufficient to define the structural features responsible for such fine-tuning of affinities, the total data confirm that the two copper binding sites in both PcoC and CopC are highly interdependent.

Because the saturated Cu^ICu^{II} form of each protein is stable in air, their properties indicate that both sites are competent to transfer copper in either oxidation state. While their specific partners in the periplasmic space are unknown, the hypersensitivity of the $\Delta pcoC$ strain of *E. coli* to copper indicates that the PcoC protein is an essential element of the resistance system.

Abbreviations: asc, ascorbate; bca, bicinchonic acid; bcs, bathocuproine disulfonate; CM, carboxymethyl; Cys or C, cysteine; DE, (diethylamino)ethyl cellulose; EDTA, *N*,*N*,*N'*,*N'*-ethylenediamine tetraacetic acid; EGTA, ethyleneglycol-*O*,*O'*-bis(2-aminoethyl)-*N*,*N*,*N'*,*N'*-tetraacetic acid; ESI-MS, electrospray ionization mass spectrometry; His or H, histidine; IPTG, isopropyl-β-D-thiogalactopyranoside; I, ionic strength; KPi, potassium phosphate buffer; MES, 2-(*N*-morpholino)ethanesulfonic acid; Met or M, methionine; OD, optical density; Phe or F, phenylalanine; Tris, tris-(hydroxymethyl)aminoethane; Trp or W, tryptophan; wt, wild type; $\square\square$, wild-type *apo*-PcoC or -CopC protein; $Cu^I\square$, Cu^I-PcoC or -CopC; $\square Cu^{II}$, Cu^{II}-PcoC or -CopC; Cu^ICu^{II}, Cu^I-Cu^{II}-PcoC or -CopC; $\square X$, *apo*-H1F variant protein; Cu^IX, Cu^I-H1F; $\square\Downarrow$, *apo*-nA-PcoC; $Cu^I\Downarrow$, Cu^I-nA-PcoC; $\square\Downarrow$, *apo*-H92F PcoC; $Cu^I\Downarrow$, Cu^I-H92F PcoC; $\Downarrow\square$, *apo*-M40L/H49F PcoC; $\Downarrow Cu^{II}$, Cu^{II}-M40L/H49F PcoC.

Supporting Information Available: PCR primer sequences (Table S1), experimental details and elution profiles of monomeric and dimeric *apo*-PcoC (Figures S1 and S2), ESI-MS data (Table S2 and Figure S3), ChemDraw structures of bcs and bca (Figure S4), Cu^{II} dissociation constants (Table S3), experimental details and Cu^I dissociation constants (Figure S5 and Table S4), UV–vis solution spectra of Cu^{II} forms of wild-type PcoC and nA-PcoC (Figure S6), and elution profiles of products of air oxidation of Cu^I-PcoC (Figure S7). This material is available free of charge via the Internet at http://pubs.acs.org.

IC070107O